

Volume 501 - 39th International Cosmic Ray Conference (ICRC2025) - Cosmic-Ray Indirect

New full-sky studies of the distribution of ultra-high-energy cosmic-ray arrival directions

A. Gálvez Ureña*, R. Higuchi, J. Kim, M. Kuznetsov, J.P. Lundquist, F.M. Mariani, *et al.* ([click to show](#))

*: *corresponding author*

Full text: [pdf](#)

Pre-published on: September 23, 2025

Published on: December 30, 2025

Abstract

Ground-based full-sky studies of the angular distribution of arrival directions of ultra-high-energy cosmic rays require combining data from different observatories, such as the Pierre Auger Observatory (Auger) and the Telescope Array (TA), because no single array can cover all declinations. A working group comprising members from the Auger and TA collaborations has been tasked with performing such studies for more than a decade and has found several indications of full-sky anisotropies. Here, we update the results for the large- and medium-scale anisotropy analyses using the latest data from TA, which include corrections for daily and yearly atmospheric effects in data for large-scale anisotropies and looser selection criteria in data for medium-scale anisotropies. We extend the latter one by considering two more galaxy catalogues, consisting of jetted or all AGNs. Finally we also introduce a new angular harmonic space analysis that allows us to measure both the auto-correlation and cross-correlation with all catalogues for all multipoles independently ($\ell_{\max} = 20$ in this work) and scanning the energy threshold.

DOI: <https://doi.org/10.22323/1.501.0282>

How to cite

Metadata are provided both in *article* format (very similar to *INSPIRE*) as this helps creating very compact bibliographies which can be beneficial to authors and readers, and in *proceeding* format which is more detailed and complete.

Open Access



Copyright owned by the author(s) under the term of the [Creative Commons Attribution-NonCommercial-NoDerivatives 4.0 International License](#).

New full-sky studies of the distribution of ultra-high-energy cosmic-ray arrival directions

A. Gálvez Ureña,^{a,*} L. Anchordoqui, M. Bianciotto, P. Biermann, T. Bister, J. Biteau, L. Caccianiga, O. Deligny, L. Deval, A. di Matteo, U. G. Giaccari, G. Golup, R. Higuchi, J. Kim, M. Kuznetsov, J. P. Lundquist, F. M. Mariani, G. Rubtsov, P. Tinyakov and F. Urban for the Pierre Auger Collaboration^{b,1} and the Telescope Array Collaboration^{c,2}

^a*CEICO—FZU, Institute of Physics of the Czech Academy of Sciences, Na Slovance 1999/2, 182 00 Prague, Czech Republic*

^b*Observatorio Pierre Auger, Av. San Martín Norte 304, 5613 Malargüe, Argentina*

^c*Telescope Array Project, 201 James Fletcher Bldg., 115 S. 1400 E., Salt Lake City, UT 84112-0830, USA*

E-mail: urena@fzu.cz, spokespersons@auger.org, ta-icrc@cosmic.utah.edu

Ground-based full-sky studies of the angular distribution of arrival directions of ultra-high-energy cosmic rays require combining data from different observatories, such as the Pierre Auger Observatory (Auger) and the Telescope Array (TA), because no single array can cover all declinations. A working group comprising members from the Auger and TA collaborations has been tasked with performing such studies for more than a decade and has found several indications of full-sky anisotropies. Here, we update the results for the large- and medium-scale anisotropy analyses using the latest data from TA, which include corrections for daily and yearly atmospheric effects in data for large-scale anisotropies and looser selection criteria in data for medium-scale anisotropies. We extend the latter one by considering two more galaxy catalogues, consisting of jetted or all AGNs. Finally we also introduce a new angular harmonic space analysis that allows us to measure both the auto-correlation and cross-correlation with all catalogues for all multipoles independently ($\ell_{\max} = 20$ in this work) and scanning the energy threshold.

*39th International Cosmic Ray Conference (ICRC 2025)
15–24 July 2025
Geneva, Switzerland*

¹Full author list: https://www.auger.org/archive/authors_icrc_2025.html

²Full author list: <http://telescopearray.org/index.php/research/collaborators>

*Speaker

1. Introduction

The most energetic particles ever measured are ultra-high-energy cosmic rays (UHECRs), which are nuclei coming from space with energies above $1 \text{ EeV} = 10^{18} \text{ eV}$. At such high energies, UHECRs interact with the cosmic microwave background (CMB) and the extragalactic background light (EBL) and quickly lose energy. This is why the sources of UHECRs must be nearby. Despite this, due to intervening magnetic fields, we do not expect the arrival direction of the particles to point back to the origin. As a result, direct association of an UHECR to its source is very challenging.

We look at large-scale anisotropies such as the dipole or quadrupole, where the effect of the magnetic fields is expected to be smaller [1]. To study larger scales, having full-sky coverage is extremely beneficial, since partial sky coverage could introduce strong degeneracies between the first few multipoles. We achieve this by combining data from the Pierre Auger Observatory (Auger) in Argentina and the Telescope Array (TA) in Utah, USA. Together they cover all declinations. Declinations $-15.7^\circ < \delta < +44.8^\circ$ are covered by both observatories, allowing us to cross-calibrate the data.

In this proceeding, we update the results of the large-scale and medium-scale anisotropy analyses that have been presented before [2, and refs. therein]. Additionally, we extend the medium-scale anisotropy analysis to two more galaxy catalogs previously used in Auger-only analyses [4], consisting of AGNs observed from the *Fermi*-LAT and *Swift*-BAT telescopes. Finally, we introduce a new angular harmonic-space analysis to search for anisotropies at large and medium scales at the highest energies.

2. The datasets

We use the latest datasets available, including events detected in Auger from 1 January 2004 to 31 December 2022 for Auger and in TA from 11 May 2008 to 10 May 2024. The Auger datasets are the same as in our previous work [2]: one with stricter cuts [3] for large-scale anisotropies, with an exposure of $123\,000 \text{ km}^2 \text{ sr yr}$, and one with looser cuts [4, but with a longer time period] for medium-scale anisotropies at the highest energies, whose exposure is $135\,000 \text{ km}^2 \text{ sr yr}$. As for TA, for large-scale anisotropies we use the same dataset as in our previous study [2], with strict cuts [5, but with a longer time period] and an effective exposure (accounting for energy resolution effects) of $19\,500 \text{ km}^2 \text{ sr yr}$, except that here for the first time we correct energy measurements for yearly and daily variations in the air density.¹ Additionally, for medium-scale anisotropies and the

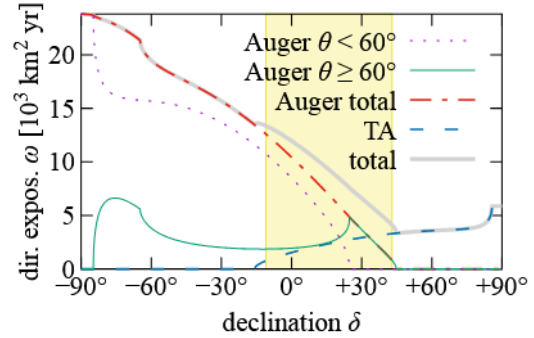


Figure 1: Directional exposures of the datasets we used for large-scale anisotropies (those for medium-scale anisotropies have the same shapes and slightly higher normalizations)

¹Namely, $E_{\text{corr}} = E_{\text{raw}} \times \left(1 - 3.5 \left(\frac{\rho}{1.042 \text{ kg/m}^3} - 1\right)\right)^{-1/1.7}$, where ρ is the air density at the TA site obtained from the Global Data Assimilation System every three hours.

angular harmonic analyses, we use looser cuts [6, but with a longer time period] for events with $E_{TA} > 57$ EeV, with 52 extra events and 5 800 km² sr yr extra exposure compared to the strict-cut dataset. See Figure 1 for the exposure of the datasets as a function of declination.

UHECR energy measurements are affected by sizeable systematic uncertainties ($\pm 14\%$ for Auger and $\pm 21\%$ for TA). This must be carefully considered, as it may have a significant impact on the results, particularly on the dipole component. We use the events in the common declination band to cross-calibrate both datasets, as in [7].² This is done by fitting the spectrum model seen in Figure 2 and the parameters α and β in:

$$E_{\text{Auger}}/10 \text{ EeV} = e^{\alpha} (E_{\text{TA}}/10 \text{ EeV})^{\beta},$$

$$E_{\text{TA}}/10 \text{ EeV} = e^{-\alpha/\beta} (E_{\text{Auger}}/10 \text{ EeV})^{1/\beta}.$$

The values obtained are $\alpha = -0.150 \pm 0.011$ and $\beta = 0.962 \pm 0.016$, resulting in

$$E_{\text{TA}} = 10 \text{ EeV} \leftrightarrow E_{\text{Auger}} = 8.60 \text{ EeV}, \quad (E_1)$$

$$E_{\text{Auger}} = 16 \text{ EeV} \leftrightarrow E_{\text{TA}} = 19.1 \text{ EeV}, \quad (E_2)$$

$$E_{\text{Auger}} = 32 \text{ EeV} \leftrightarrow E_{\text{TA}} = 39.2 \text{ EeV}. \quad (E_3)$$

In the dataset used for large-scale anisotropies, there are 43 600 Auger events with $E \geq E_1$, of which 13 027 with $E \geq E_2$ and 2 739 with $E \geq E_3$, and 6 611 TA events with $E \geq E_1$, of which 1 967 with $E \geq E_2$ and 484 with $E \geq E_3$. The flux distribution in this dataset in the three energy bins is shown in Figure 3.

As previously mentioned, for the intermediate scale anisotropies and the harmonic analyses we use the TA loose-cut data for $E_{TA} \geq 57$ EeV. However, since this dataset does not have available atmospheric corrections, we use the energy calibration from [2], with $\alpha = -0.159$, $\beta = 0.954$, and $E_{\text{Auger}} = 32 \text{ EeV} \leftrightarrow E_{\text{TA}} = 40.0 \text{ EeV}$. We have 2 936 Auger events above 32 EeV and 513 TA events above 40.0 EeV (of which 285 TA strict-cut events with $40.0 \text{ EeV} \leq E_{TA} < 57 \text{ EeV}$ and 228 TA loose-cut events with $E_{TA} \geq 57 \text{ EeV}$).

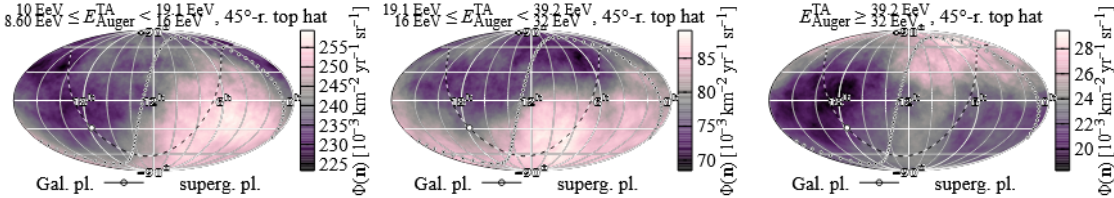


Figure 3: The flux distribution of the dataset we use for large-scale anisotropies (equatorial coordinates, Mollweide projection), smoothed by a 45°-radius top-hat window

²This cross-calibration is optimized for anisotropy studies and should not be used outside of the scope of this analysis.

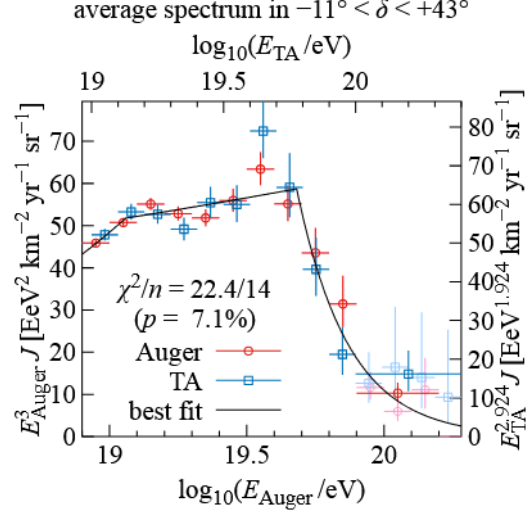


Figure 2: The spectrum fit to the two datasets in order to obtain a mapping between Auger and TA energy scales. The highest-energy bins of each dataset (denoted by thin pale lines) are combined into one larger bin (denoted by regular lines) to ensure the probability distribution can be approximated as log-normal.

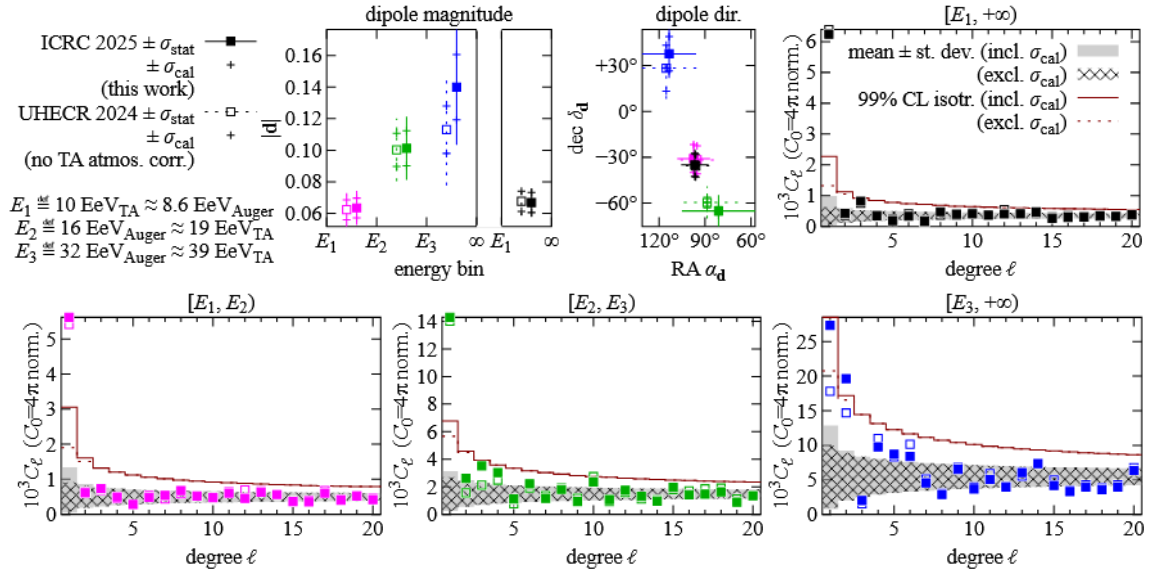


Figure 4: The first and second panels show how the magnitude and direction of the dipole have changed with the inclusion of TA atmospheric corrections; the next ones show how the harmonic space auto-correlation (also known as angular power spectrum) has changed in the different energy bins used.

3. Large-scale analysis

Given our data map of UHECRs, we can expand it in spherical harmonics as

$$M(\mathbf{n}) = \sum_{\ell=0}^{\infty} \sum_{m=-\ell}^{+\ell} a_{\ell m} Y_{\ell m}(\mathbf{n}) \rightarrow a_{\ell m} = \int d\Omega Y_{\ell m}(\mathbf{n}) M(\mathbf{n}).$$

The $\ell = 1$ contribution can be expressed as a dipole vector $\mathbf{d} = \sqrt{3}(a_{11}, a_{1-1}, a_{10})$, its direction and magnitude shown in the first two plots of Figure 4. Since we have a full-sky dataset, we can directly measure $a_{\ell m} = \sum_{\text{evt}} Y_{\ell m}(\mathbf{n}_{\text{evt}})/\omega(\mathbf{n}_{\text{evt}})$, where ω is the total directional exposure of the combined dataset. We perform the analysis in three energy bins $[E_1, E_2]$, $[E_2, E_3]$, $[E_3, +\infty)$ as defined in the previous section plus a cumulative bin $[E_3, +\infty)$. The results are shown in Figure 4, and compared with our previous results [2] using the same time periods but without TA atmospheric corrections. The dipole and quadrupole in the highest energy bin have become stronger, but still not particularly significant, respectively at $p = 0.011$ (2.5σ) and $p = 0.0041$ (2.9σ) pre-trial. All results are otherwise similar to the previous ones.

The dipole direction in the cumulative bin is 92° away from the Galactic Centre. A hint of a quadrupole along the supergalactic plane is found in the highest energy bin, motivating section 5.

4. Intermediate-scale analysis

This analysis must be performed at the highest energies, where the deflections due to magnetic fields are expected to be smaller. We perform targeted searches using four source catalogues [4]:

- 44 113 galaxies of all types, based on the 2MASS catalogue, weighted by their near-IR fluxes;

- 44 starburst galaxies, based on the Lunardini catalogue, weighted by their radio fluxes;
- 523 AGNs, based on the *Swift*-BAT catalogue, weighted by their X-ray fluxes; and
- 26 jetted AGNs, from the *Fermi*-LAT catalogue, weighted by their gamma-ray fluxes.

For more details about the data sources, selection criteria, and weights used for compiling these catalogues see [4]. All these catalogues include galaxies with distances $1 \text{ Mpc} \leq D < 250 \text{ Mpc}$, except the starburst galaxy one, which includes galaxies with distances $1 \text{ Mpc} \leq D < 130 \text{ Mpc}$.

We then define the test statistics

$$\text{TS}(\Theta, f, E_{\min}) = 2 \ln \left(\frac{\mathcal{L}(\Theta, f, E_{\min})}{\mathcal{L}(\Theta, f = 0, E_{\min})} \right), \quad \mathcal{L}(\Theta, f, E_{\min}) = \prod_{E_i > E_{\min}} \frac{\Phi(\hat{\mathbf{n}}_i, \Theta, f) \omega(\hat{\mathbf{n}}_i, E_i)}{\int_{4\pi} d\Omega \Phi(\hat{\mathbf{n}}, \Theta, f) \omega(\hat{\mathbf{n}}, E_i)}.$$

Here, i refers to the i -th UHECR, while the weight $\omega(\hat{\mathbf{n}}, E)$ is the directional exposure, which (unlike in our previous studies [2, 4]) is also a function of the energy because a TA dataset with stricter cuts is used for $40 \text{ EeV} \leq E_{\text{TA}} < 57 \text{ EeV}$ but one with looser cuts, hence larger exposure, is used for $E_{\text{TA}} \geq 57 \text{ EeV}$; and $\Phi(\hat{\mathbf{n}}_i, \Theta, f)$ is defined as:

$$\Phi(\hat{\mathbf{n}}, \Theta, f) := f \Phi_{\text{signal}}(\hat{\mathbf{n}}, \Theta) + (1 - f) \Phi_{\text{background}},$$

where the background contribution is isotropic and the signal contribution is a sum of von Mises–Fisher distributions for each source

$$\Phi_{\text{signal}}(\hat{\mathbf{n}}, \Theta) := \frac{1}{\sum_s a(D_s, E_{\min}) w_s} \sum_s \frac{a(D_s, E_{\min}) w_s \Theta^{-2}}{4\pi \sinh(\Theta^{-2})} e^{\Theta^{-2} \hat{\mathbf{n}}_s \cdot \hat{\mathbf{n}}}, \quad \Phi_{\text{background}} := \frac{1}{4\pi},$$

where the index s runs over sources in the galaxy catalogue, w_s is the flux of the s -th source, and $a(D_s, E_{\min})$ is the attenuation, computed as in [4] following the best fit to Auger data above the ankle energy [8] assuming the EPOS LHC hadronic interaction model, with a mixed mass composition (67.3% He, 28.1% N and 4.6% Si at $E = 1 \text{ EeV}$) and a relatively hard spectrum ($\propto E^{-0.96} \exp(-R/10^{18.68} \text{ V})$ where $R = E/Z$) at injection.

The analysis is repeated for increasing energy thresholds, $E_{\text{Auger}} = 32 \text{ EeV}, 33 \text{ EeV}, \dots, 80 \text{ EeV}$. The results are presented in Figure 5. The details of the maximum TS for each galaxy catalogue are shown in Table 1. To allow a direct comparison to our previous results [2] where the TA loose-cut data were not used, in the case of the all-galaxy and starburst galaxy catalogues we also shown results obtained neglecting the attenuation.

5. Angular Harmonic Space Analysis

For this analysis we combine the Harmonic Auto-Correlation as calculated in section 3 with the energy scanning from section 4. We also perform the same analysis with Harmonic Cross-Correlation of the UHECR map and the galaxy catalogues introduced in the previous section (including the attenuations). The Cross-Correlation is a valuable tool as it inherently involves more information than the Auto-Correlation, making it more likely to break possible degeneracies. Furthermore, for the Cross-Correlation the statistical and systematic noises do not correlate, resulting in a clearer signal. In the case in which the number of sources in the catalogue is much bigger than

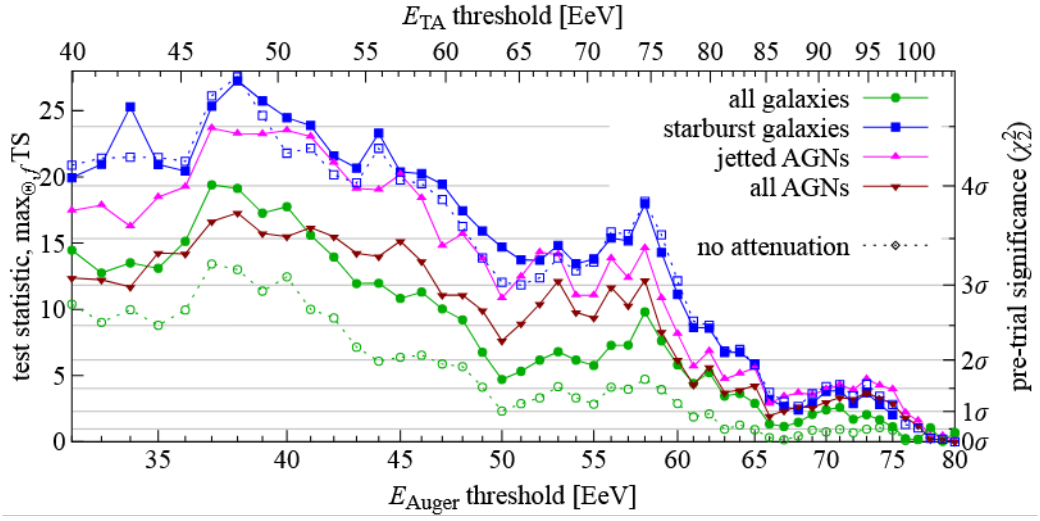


Figure 5: Significances of the correlations with galaxy catalogues as a function of the energy threshold.

	E_{\min}	TS	$f/\%$	$\Theta/^\circ$	post-trial
All galaxies	$37 \text{ EeV}_{\text{Auger}} \approx 47 \text{ EeV}_{\text{TA}}$	19.3	$13.1^{+4.7}_{-3.6}$	$15.5^{+6.1}_{-3.6}$	3.4σ
Starburst galaxies	$38 \text{ EeV}_{\text{Auger}} \approx 48 \text{ EeV}_{\text{TA}}$	27.3	$10.6^{+56.6}_{-3.2}$	$17.6^{+26.6}_{-4.1}$	4.2σ
All AGNs	$38 \text{ EeV}_{\text{Auger}} \approx 48 \text{ EeV}_{\text{TA}}$	17.6	$4.8^{+1.6}_{-1.4}$	$15.4^{+3.5}_{-2.8}$	3.3σ
Jetted AGNs	$37 \text{ EeV}_{\text{Auger}} \approx 47 \text{ EeV}_{\text{TA}}$	22.9	$8.8^{+2.6}_{-2.3}$	$17.4^{+3.4}_{-2.8}$	3.8σ
All gal. (no atten.)	$37 \text{ EeV}_{\text{Auger}} \approx 47 \text{ EeV}_{\text{TA}}$	13.5	$33.6^{+26.3}_{-19.4}$	$29.2^{+12.9}_{-17.5}$	2.8σ
Starburst gal. (no atten.)	$38 \text{ EeV}_{\text{Auger}} \approx 48 \text{ EeV}_{\text{TA}}$	27.3	$10.6^{+4.0}_{-2.7}$	$15.0^{+4.8}_{-2.9}$	4.2σ

Table 1: Best fit of the medium-scale analysis for each of the galaxy catalogues considered. We show both the optimal parameters and the TS that was achieved, as well as the corresponding one-tailed post-trial significance. The reasons for the increase in the upper uncertainties on f and Θ when including the attenuation in the starburst galaxy catalogue are under investigation.

the number of cosmic rays (like is the case for the all-galaxy catalogue), the shot noise is greatly reduced, for more details see [10].

Both the Harmonic Auto-Correlation of the UHECRs and their Cross-Correlation with the different galaxy catalogues can be obtained for any multipole following section 3 and using

$$C_l^{\text{CR CR}} := \frac{1}{2\ell+1} \sum_{m=-\ell}^{+\ell} a_{lm}^{\text{CR}} a_{lm}^{*\text{CR}}, \quad C_l^{\text{CR Cat}} := \frac{1}{2\ell+1} \sum_{m=-\ell}^{+\ell} a_{lm}^{\text{CR}} a_{lm}^{*\text{Cat}}.$$

For the Cross-Correlation, the map used includes the attenuation discussed in section 4. Then, using isotropic simulations, we can obtain the pre-trial significance of each multipole (we consider $\ell_{\max} = 20$ in this work). To reduce computational time, it is assumed that isotropic

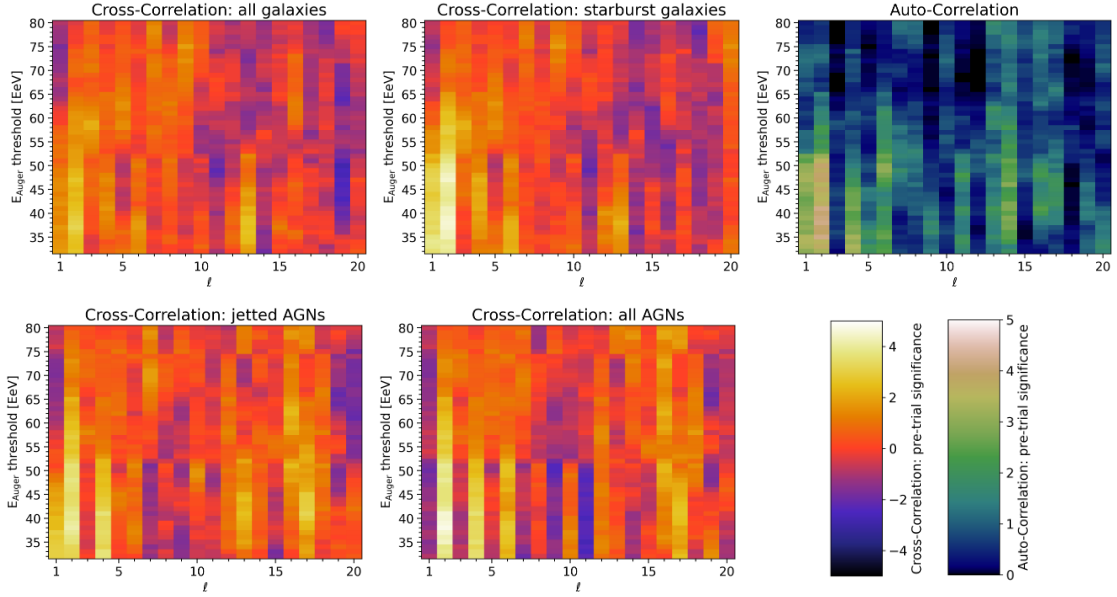


Figure 6: Pre-trial significances for each multipole order and energy threshold of the Auto-Correlation and the Cross-Correlation with all galaxies, starburst galaxies, jetted AGNs and all AGNs.

Cross-Correlations follow a Gaussian distribution, while the Auto-Correlations follow [9]:

$$f(\bar{C}_\ell^{\text{CR CR}} | C_\ell^{\text{CR CR}}) \propto C_\ell^{\text{CR CR}} \left(\frac{\bar{C}_\ell^{\text{CR CR}}}{C_\ell^{\text{CR CR}}} \right)^{\frac{2\ell+1}{2}-1} \exp\left(-\frac{(2\ell+1)\bar{C}_\ell^{\text{CR CR}}}{2} C_\ell^{\text{CR CR}}\right),$$

where $\bar{C}_\ell^{\text{CR CR}}$ is expected value for isotropy, given by the average of all simulations. We can then calculate the p -value of a data point $C_{\ell, \text{Data}}^{\text{CR CR}}$ as

$$p\text{-value} = 1 - \frac{\int_0^{C_{\ell, \text{Data}}^{\text{CR CR}}} dC_\ell^{\text{CR CR}} f(\bar{C}_\ell^{\text{CR CR}} | C_\ell^{\text{CR CR}})}{\int_0^\infty dC_\ell^{\text{CR CR}} f(\bar{C}_\ell^{\text{CR CR}} | C_\ell^{\text{CR CR}})},$$

and equivalently for the cross-correlation, for which the function f would be a Gaussian with mean and standard deviation calculated directly from the isotropic simulations. Then the analysis is repeated for increasing energy thresholds as in section 4. For the Cross-Correlations we use the same galaxy catalogues as in section 4.

The results are shown in Figure 6. From this figure we see that the quadrupole is the most statistically significant multipole in all cases. We then find the energy threshold at which the quadrupole is the most significant in each plot of Figure 6 and obtain a corresponding post-trial significance. For this we follow the most conservative approach, by taking into account the scan in energy and the measurements of different mutipoles up to $\ell = 20$. The results for this analysis are then presented in Table 2.

6. Conclusions

We have presented an update to our previous analyses and introduced a new one. For the analysis on large angular scales, we have incorporated new atmospheric corrections to the energy

	ℓ	E_{\min}	pre-trial	post-trial
Auto-Correlation	2	41 EeV _{Auger} \approx 51.8 EeV _{TA}	4.2 σ	2.1 σ
All galaxies	2	37 EeV _{Auger} \approx 46.5 EeV _{TA}	3.2 σ	—
Starburst galaxies	2	38 EeV _{Auger} \approx 47.8 EeV _{TA}	4.5 σ	2.7 σ
All AGNs	2	38 EeV _{Auger} \approx 47.8 EeV _{TA}	4.7 σ	3.0 σ
Jetted AGNs	2	38 EeV _{Auger} \approx 47.8 EeV _{TA}	4.1 σ	2.0 σ

Table 2: We show the ℓ and E_{\min} at which the maximum significance is obtained for the Auto-Correlation and for the Cross-Correlation with each galaxy catalogue. We present the pre-trial maximum obtained and the post-trial result calculated from it.

of the TA data. Most of our results remain similar, except for those at the highest energies, where the dipole and quadrupole have become more significant (but within the statistical uncertainties).

For our intermediate-scale analysis, we have introduced new data from the TA side, using a dataset with looser cuts at the highest energies. For the first time in full-sky analyses, we have also taken into account the energy losses of UHECRs. Furthermore, we have extended the analysis to include two more source catalogues. The correlation with starburst galaxies remains the most significant, at 4.2 σ post-trial, even after the inclusion of attenuations, which primarily enhanced the correlation with the all-galaxy catalogue.

Finally, we have studied the harmonic autocorrelation and cross-correlation methods. Our results show that, given an appropriate source catalogue, the cross-correlation can yield a clearer signal than the harmonic auto-correlation. As a next step, we plan to investigate how to combine auto- and cross-correlations, or how to merge different multipoles to enhance statistical significance. In the future, the method introduced here could serve as a robust tool for source matching, less sensitive to the specific characteristics of the Galactic magnetic field.

References

- [1] A. di Matteo and P. Tinyakov, *MNRAS* **476** (2018) 715 [1706.02534].
- [2] G. Rubtsov et al. [for the Pierre Auger and Telescope Array collabs.], *PoS (UHECR2024)* 009.
- [3] A. Abdul Halim et al. [Pierre Auger collab.], *ApJ* **976** (2024) 48 [2408.05292].
- [4] P. Abreu et al. [Pierre Auger collab.], *ApJ* **935** (2022) 170 [2206.13492].
- [5] A. Aab et al. [Pierre Auger and Telescope Array collabs.], *ApJ* **794** (2014) 172 [1409.3128].
- [6] R.U. Abbasi et al. [Telescope Array collab.], *ApJL* **790** (2014) L21 [1404.5890].
- [7] P. Tinyakov et al. [for the Pierre Auger and Telescope Array collabs.], *PoS (ICRC2021)* 375.
- [8] A. Aab et al. [Pierre Auger collab.], *JCAP* **04** (2017) 038 [1612.07155].
- [9] W.J. Percival and M.L. Brown, *MNRAS* **372** (2006) 1104 [astro-ph/0604547].
- [10] F.R. Urban, S. Camera and D. Alonso, *A&A* **652** (2021) A41 [2005.00244].

The Pierre Auger Collaboration



**PIERRE
AUGER**
OBSERVATORY

A. Abdul Halim¹³, P. Abreu⁷⁰, M. Aglietta^{53,51}, I. Allekotte¹, K. Almeida Cheminant^{78,77}, A. Almela^{7,12}, R. Aloisio^{44,45}, J. Alvarez-Muñiz⁷⁶, A. Ambrosone⁴⁴, J. Ammerman Yebra⁷⁶, G.A. Anastasi^{57,46}, L. Anchordoqui⁸³, B. Andrada⁷, L. Andrade Dourado^{44,45}, S. Andringa⁷⁰, L. Apollonio^{58,48}, C. Aramo⁴⁹, E. Arnone^{62,51}, J.C. Arteaga Velázquez⁶⁶, P. Assis⁷⁰, G. Avila¹¹, E. Avocone^{56,45}, A. Bakalova³¹, F. Barbato^{44,45}, A. Bartz Mocellin⁸², J.A. Bellido¹³, C. Berat³⁵, M.E. Bertaina^{62,51}, M. Bianciotto^{62,51}, P.L. Biermann^a, V. Binet⁵, K. Bismark^{38,7}, T. Bister^{77,78}, J. Biteau^{36,i}, J. Blazek³¹, J. Blümer⁴⁰, M. Boháčová³¹, D. Boncioli^{56,45}, C. Bonifazi⁸, L. Bonneau Arbeletche²², N. Borodai⁶⁸, J. Brack^f, P.G. Bricchetto Orchera^{7,40}, F.L. Briechle⁴¹, A. Bueno⁷⁵, S. Buitink¹⁵, M. Buscemi^{46,57}, M. Büsken^{38,7}, A. Bwembya^{77,78}, K.S. Caballero-Mora⁶⁵, S. Cabana-Freire⁷⁶, L. Caccianiga^{58,48}, F. Campuzano⁶, J. Caraça-Valente⁸², R. Caruso^{57,46}, A. Castellina^{53,51}, F. Catalani¹⁹, G. Cataldi⁴⁷, L. Cazon⁷⁶, M. Cerda¹⁰, B. Čermáková⁴⁰, A. Cerumenati^{44,45}, J.A. Chinellato²², J. Chudoba³¹, L. Chytka³², R.W. Clay¹³, A.C. Cobos Cerutti⁶, R. Colalillo^{59,49}, R. Conceição⁷⁰, G. Consolati^{48,54}, M. Conte^{55,47}, F. Convenga^{44,45}, D. Correia dos Santos²⁷, P.J. Costa⁷⁰, C.E. Covault⁸¹, M. Cristinziani⁴³, C.S. Cruz Sanchez³, S. Dasso^{4,2}, K. Daumiller⁴⁰, B.R. Dawson¹³, R.M. de Almeida²⁷, E.-T. de Boone⁴³, B. de Errico²⁷, J. de Jesús⁷, S.J. de Jong^{77,78}, J.R.T. de Mello Neto²⁷, I. De Mitri^{44,45}, J. de Oliveira¹⁸, D. de Oliveira Franco⁴², F. de Palma^{55,47}, V. de Souza²⁰, E. De Vito^{55,47}, A. Del Popolo^{57,46}, O. Deligny³³, N. Denner³¹, L. Deval^{53,51}, A. di Matteo⁵¹, C. Dobrigkeit²², J.C. D'Olivo⁶⁷, L.M. Domingues Mendes^{16,70}, Q. Dorosti⁴³, J.C. dos Anjos¹⁶, R.C. dos Anjos²⁶, J. Ebr³¹, F. Ellwanger⁴⁰, R. Engel^{38,40}, I. Epicoco^{55,47}, M. Erdmann⁴¹, A. Etchegoyen^{7,12}, C. Evoli^{44,45}, H. Falcke^{77,79,78}, G. Farrar⁸⁵, A.C. Fauth²², T. Fehler⁴³, F. Feldbusch³⁹, A. Fernandes⁷⁰, M. Fernandez¹⁴, B. Fick⁸⁴, J.M. Figueira⁷, P. Filip^{38,7}, A. Filipčič^{74,73}, T. Fitoussi⁴⁰, B. Flagg⁸⁷, T. Fodran⁷⁷, A. Franco⁴⁷, M. Freitas⁷⁰, T. Fujii^{86,h}, A. Fuster^{7,12}, C. Galea⁷⁷, B. García⁶, C. Gaudu³⁷, P.L. Ghia³³, U. Giaccari⁴⁷, F. Gobbi¹⁰, F. Gollan⁷, G. Golup¹, M. Gómez Berisso¹, P.F. Gómez Vitale¹¹, J.P. Gongora¹¹, J.M. González¹, N. González⁷, D. Góra⁶⁸, A. Gorgi^{53,51}, M. Gottowik⁴⁰, F. Guarino^{59,49}, G.P. Guedes²³, L. Gülzow⁴⁰, S. Hahn³⁸, P. Hamal³¹, M.R. Hampel⁷, P. Hansen³, V.M. Harvey¹³, A. Haungs⁴⁰, T. Hebbeker⁴¹, C. Hojvat^d, J.R. Hörandel^{77,78}, P. Horvath³², M. Hrabovský³², T. Huege^{40,15}, A. Insolia^{57,46}, P.G. Isar⁷², M. Ismaiel^{77,78}, P. Janecek³¹, V. Jilek³¹, K.-H. Kampert³⁷, B. Keilhauer⁴⁰, A. Khakurdikar⁷⁷, V.V. Kizakke Covilakam^{7,40}, H.O. Klages⁴⁰, M. Kleifges³⁹, J. Köhler⁴⁰, F. Krieger⁴¹, M. Kubatova³¹, N. Kunka³⁹, B.L. Lago¹⁷, N. Langner⁴¹, N. Leal⁷, M.A. Leigui de Oliveira²⁵, Y. Lema-Capeans⁷⁶, A. Letessier-Selvon³⁴, I. Lhenry-Yvon³³, L. Lopes⁷⁰, J.P. Lundquist⁷³, M. Mallamaci^{60,46}, D. Mandat³¹, P. Mantsch^d, F.M. Mariani^{58,48}, A.G. Mariazzi³, I.C. Mariş¹⁴, G. Marsella^{60,46}, D. Martello^{55,47}, S. Martinelli^{40,7}, M.A. Martins⁷⁶, H.-J. Mathes⁴⁰, J. Matthews^g, G. Matthiae^{61,50}, E. Mayotte⁸², S. Mayotte⁸², P.O. Mazur^d, G. Medina-Tanco⁶⁷, J. Meinert³⁷, D. Melo⁷, A. Menshikov³⁹, C. Merx⁴⁰, S. Michal³¹, M.I. Micheletti⁵, L. Miramonti^{58,48}, M. Mogarkar⁶⁸, S. Mollerach¹, F. Montanet³⁵, L. Morejon³⁷, K. Mulrey^{77,78}, R. Mussa⁵¹, W.M. Namasaka³⁷, S. Negi³¹, L. Nellen⁶⁷, K. Nguyen⁸⁴, G. Nicora⁹, M. Niechciol⁴³, D. Nitz⁸⁴, D. Nosek³⁰, A. Novikov⁸⁷, V. Novotny³⁰, L. Nožka³², A. Nucita^{55,47}, L.A. Núñez²⁹, J. Ochoa^{7,40}, C. Oliveira²⁰, L. Östman³¹, M. Palatka³¹, J. Pallotta⁹, S. Panja³¹, G. Parente⁷⁶, T. Paulsen³⁷, J. Pawlowsky³⁷, M. Pech³¹, J. Pękala⁶⁸, R. Pelayo⁶⁴, V. Pelgrims¹⁴, L.A.S. Pereira²⁴, E.E. Pereira Martins^{38,7}, C. Pérez Bertolli^{7,40}, L. Perrone^{55,47}, S. Petrerá^{44,45}, C. Petrucci⁵⁶, T. Pierog⁴⁰, M. Pimenta⁷⁰, M. Platino⁷, B. Pont⁷⁷, M. Pourmohammad Shahvar^{60,46}, P. Privitera⁸⁶, C. Priyadarshi⁶⁸, M. Prouza³¹, K. Pytel⁶⁹, S. Querschfeld³⁷, J. Rautenberg³⁷, D. Ravnani⁷, J.V. Reginatto Akim²², A. Reuzki⁴¹, J. Ridky³¹, F. Riehn^{76,j}, M. Risse⁴³, V. Rizi^{56,45}, E. Rodriguez^{7,40}, G. Rodriguez Fernandez⁵⁰, J. Rodriguez Rojo¹¹, S. Rossoni⁴², M. Roth⁴⁰, E. Roulet¹, A.C. Rovero⁴, A. Saftoiu⁷¹, M. Saharan⁷⁷, F. Salamida^{56,45}, H. Salazar⁶³, G. Salina⁵⁰, P. Sampathkumar⁴⁰, N. San Martin⁸², J.D. Sanabria Gomez²⁹, F. Sánchez⁷, E.M. Santos²¹, E. Santos³¹, F. Sarazin⁸², R. Sarmento⁷⁰, R. Sato¹¹, P. Savina^{44,45}, V. Scherini^{55,47}, H. Schieler⁴⁰, M. Schimassek³³, M. Schimp³⁷, D. Schmidt⁴⁰, O. Scholten^{15,b}, H. Schoorlemmer^{77,78}, P. Schovánek³¹, F.G. Schröder^{87,40}, J. Schulte⁴¹, T. Schulz³¹, S.J. Sciutto³, M. Scornavacche⁷, A. Sedoski⁷, A. Segreto^{52,46}, S. Sehgal³⁷, S.U. Shivashankara⁷³, G. Sigl⁴², K. Simkova^{15,14}, F. Simon³⁹, R. Šmída⁸⁶, P. Sommers^e, R. Squartini¹⁰, M. Stadelmaier^{40,48,58}, S. Stanič⁷³, J. Stasielak⁶⁸, P. Stassi³⁵, S. Strähz³⁸, M. Straub⁴¹, T. Suomijärvi³⁶, A.D. Supanitsky⁷, Z. Svozilikova³¹, K. Syrovkas³⁰, Z. Szadkowski⁶⁹, F. Tairli¹³, M. Tambone^{59,49}, A. Tapia²⁸, C. Taricco^{62,51}, C. Timmermans^{78,77}, O. Tkachenko³¹, P. Tobiska³¹, C.J. Toderó Peixoto¹⁹, B. Tomé⁷⁰, A. Travaini¹⁰, P. Travnicek³¹, M. Tüeros³, M. Unger⁴⁰, R. Uzeiroska³⁷, L. Vaclavek³², M. Vacula³², I. Vaiman^{44,45}, J.F. Valdés Galicia⁶⁷, L. Valore^{59,49}, P. van Dillen^{77,78}, E. Varela⁶³, V. Vašíčková³⁷, A. Vásquez-Ramírez²⁹, D. Veberič⁴⁰, I.D. Vergara Quispe³, S. Verpoest⁸⁷, V. Verzi⁵⁰, J. Vicha³¹, J. Vink⁸⁰, S. Vorobiov⁷³, J.B. Vuta³¹, C. Watanabe²⁷, A.A. Watson^c, A. Weindl⁴⁰, M. Weitz³⁷, L. Wiencke⁸², H. Wilczyński⁶⁸, B. Wundheiler⁷, B. Yue³⁷, A. Yushkov³¹, E. Zas⁷⁶, D. Zavrtanik^{73,74}, M. Zavrtanik^{74,73}

- ¹ Centro Atómico Bariloche and Instituto Balseiro (CNEA-UNCuyo-CONICET), San Carlos de Bariloche, Argentina
- ² Departamento de Física and Departamento de Ciencias de la Atmósfera y los Océanos, FCEyN, Universidad de Buenos Aires and CONICET, Buenos Aires, Argentina
- ³ IFLP, Universidad Nacional de La Plata and CONICET, La Plata, Argentina
- ⁴ Instituto de Astronomía y Física del Espacio (IAFE, CONICET-UBA), Buenos Aires, Argentina
- ⁵ Instituto de Física de Rosario (IFIR) – CONICET/U.N.R. and Facultad de Ciencias Bioquímicas y Farmacéuticas U.N.R., Rosario, Argentina
- ⁶ Instituto de Tecnologías en Detección y Astropartículas (CNEA, CONICET, UNSAM), and Universidad Tecnológica Nacional – Facultad Regional Mendoza (CONICET/CNEA), Mendoza, Argentina
- ⁷ Instituto de Tecnologías en Detección y Astropartículas (CNEA, CONICET, UNSAM), Buenos Aires, Argentina
- ⁸ International Center of Advanced Studies and Instituto de Ciencias Físicas, ECyT-UNSAM and CONICET, Campus Miguelete – San Martín, Buenos Aires, Argentina
- ⁹ Laboratorio Atmósfera – Departamento de Investigaciones en Láseres y sus Aplicaciones – UNIDEF (CITEDEF-CONICET), Argentina
- ¹⁰ Observatorio Pierre Auger, Malargüe, Argentina
- ¹¹ Observatorio Pierre Auger and Comisión Nacional de Energía Atómica, Malargüe, Argentina
- ¹² Universidad Tecnológica Nacional – Facultad Regional Buenos Aires, Buenos Aires, Argentina
- ¹³ University of Adelaide, Adelaide, S.A., Australia
- ¹⁴ Université Libre de Bruxelles (ULB), Brussels, Belgium
- ¹⁵ Vrije Universiteit Brussels, Brussels, Belgium
- ¹⁶ Centro Brasileiro de Pesquisas Físicas, Rio de Janeiro, RJ, Brazil
- ¹⁷ Centro Federal de Educação Tecnológica Celso Suckow da Fonseca, Petropolis, Brazil
- ¹⁸ Instituto Federal de Educação, Ciência e Tecnologia do Rio de Janeiro (IFRJ), Brazil
- ¹⁹ Universidade de São Paulo, Escola de Engenharia de Lorena, Lorena, SP, Brazil
- ²⁰ Universidade de São Paulo, Instituto de Física de São Carlos, São Carlos, SP, Brazil
- ²¹ Universidade de São Paulo, Instituto de Física, São Paulo, SP, Brazil
- ²² Universidade Estadual de Campinas (UNICAMP), IFGW, Campinas, SP, Brazil
- ²³ Universidade Estadual de Feira de Santana, Feira de Santana, Brazil
- ²⁴ Universidade Federal de Campina Grande, Centro de Ciências e Tecnologia, Campina Grande, Brazil
- ²⁵ Universidade Federal do ABC, Santo André, SP, Brazil
- ²⁶ Universidade Federal do Paraná, Setor Palotina, Palotina, Brazil
- ²⁷ Universidade Federal do Rio de Janeiro, Instituto de Física, Rio de Janeiro, RJ, Brazil
- ²⁸ Universidad de Medellín, Medellín, Colombia
- ²⁹ Universidad Industrial de Santander, Bucaramanga, Colombia
- ³⁰ Charles University, Faculty of Mathematics and Physics, Institute of Particle and Nuclear Physics, Prague, Czech Republic
- ³¹ Institute of Physics of the Czech Academy of Sciences, Prague, Czech Republic
- ³² Palacky University, Olomouc, Czech Republic
- ³³ CNRS/IN2P3, IJCLab, Université Paris-Saclay, Orsay, France
- ³⁴ Laboratoire de Physique Nucléaire et de Hautes Energies (LPNHE), Sorbonne Université, Université de Paris, CNRS-IN2P3, Paris, France
- ³⁵ Univ. Grenoble Alpes, CNRS, Grenoble Institute of Engineering Univ. Grenoble Alpes, LPSC-IN2P3, 38000 Grenoble, France
- ³⁶ Université Paris-Saclay, CNRS/IN2P3, IJCLab, Orsay, France
- ³⁷ Bergische Universität Wuppertal, Department of Physics, Wuppertal, Germany
- ³⁸ Karlsruhe Institute of Technology (KIT), Institute for Experimental Particle Physics, Karlsruhe, Germany
- ³⁹ Karlsruhe Institute of Technology (KIT), Institut für Prozessdatenverarbeitung und Elektronik, Karlsruhe, Germany
- ⁴⁰ Karlsruhe Institute of Technology (KIT), Institute for Astroparticle Physics, Karlsruhe, Germany
- ⁴¹ RWTH Aachen University, III. Physikalisches Institut A, Aachen, Germany
- ⁴² Universität Hamburg, II. Institut für Theoretische Physik, Hamburg, Germany
- ⁴³ Universität Siegen, Department Physik – Experimentelle Teilchenphysik, Siegen, Germany
- ⁴⁴ Gran Sasso Science Institute, L'Aquila, Italy
- ⁴⁵ INFN Laboratori Nazionali del Gran Sasso, Assergi (L'Aquila), Italy
- ⁴⁶ INFN, Sezione di Catania, Catania, Italy
- ⁴⁷ INFN, Sezione di Lecce, Lecce, Italy
- ⁴⁸ INFN, Sezione di Milano, Milano, Italy
- ⁴⁹ INFN, Sezione di Napoli, Napoli, Italy
- ⁵⁰ INFN, Sezione di Roma “Tor Vergata”, Roma, Italy
- ⁵¹ INFN, Sezione di Torino, Torino, Italy

- 52 Istituto di Astrofisica Spaziale e Fisica Cosmica di Palermo (INAF), Palermo, Italy
 53 Osservatorio Astrofisico di Torino (INAF), Torino, Italy
 54 Politecnico di Milano, Dipartimento di Scienze e Tecnologie Aerospaziali, Milano, Italy
 55 Università del Salento, Dipartimento di Matematica e Fisica “E. De Giorgi”, Lecce, Italy
 56 Università dell’Aquila, Dipartimento di Scienze Fisiche e Chimiche, L’Aquila, Italy
 57 Università di Catania, Dipartimento di Fisica e Astronomia “Ettore Majorana”, Catania, Italy
 58 Università di Milano, Dipartimento di Fisica, Milano, Italy
 59 Università di Napoli “Federico II”, Dipartimento di Fisica “Ettore Pancini”, Napoli, Italy
 60 Università di Palermo, Dipartimento di Fisica e Chimica “E. Segrè”, Palermo, Italy
 61 Università di Roma “Tor Vergata”, Dipartimento di Fisica, Roma, Italy
 62 Università Torino, Dipartimento di Fisica, Torino, Italy
 63 Benemérita Universidad Autónoma de Puebla, Puebla, México
 64 Unidad Profesional Interdisciplinaria en Ingeniería y Tecnologías Avanzadas del Instituto Politécnico Nacional (UPIITA-IPN), México, D.F., México
 65 Universidad Autónoma de Chiapas, Tuxtla Gutiérrez, Chiapas, México
 66 Universidad Michoacana de San Nicolás de Hidalgo, Morelia, Michoacán, México
 67 Universidad Nacional Autónoma de México, México, D.F., México
 68 Institute of Nuclear Physics PAN, Krakow, Poland
 69 University of Łódź, Faculty of High-Energy Astrophysics, Łódź, Poland
 70 Laboratório de Instrumentação e Física Experimental de Partículas – LIP and Instituto Superior Técnico – IST, Universidade de Lisboa – UL, Lisboa, Portugal
 71 “Horia Hulubei” National Institute for Physics and Nuclear Engineering, Bucharest-Magurele, Romania
 72 Institute of Space Science, Bucharest-Magurele, Romania
 73 Center for Astrophysics and Cosmology (CAC), University of Nova Gorica, Nova Gorica, Slovenia
 74 Experimental Particle Physics Department, J. Stefan Institute, Ljubljana, Slovenia
 75 Universidad de Granada and C.A.F.P.E., Granada, Spain
 76 Instituto Galego de Física de Altas Enerxías (IGFAE), Universidade de Santiago de Compostela, Santiago de Compostela, Spain
 77 IMAPP, Radboud University Nijmegen, Nijmegen, The Netherlands
 78 Nationaal Instituut voor Kernfysica en Hoge Energie Fysica (NIKHEF), Science Park, Amsterdam, The Netherlands
 79 Stichting Astronomisch Onderzoek in Nederland (ASTRON), Dwingeloo, The Netherlands
 80 Universiteit van Amsterdam, Faculty of Science, Amsterdam, The Netherlands
 81 Case Western Reserve University, Cleveland, OH, USA
 82 Colorado School of Mines, Golden, CO, USA
 83 Department of Physics and Astronomy, Lehman College, City University of New York, Bronx, NY, USA
 84 Michigan Technological University, Houghton, MI, USA
 85 New York University, New York, NY, USA
 86 University of Chicago, Enrico Fermi Institute, Chicago, IL, USA
 87 University of Delaware, Department of Physics and Astronomy, Bartol Research Institute, Newark, DE, USA

^a Max-Planck-Institut für Radioastronomie, Bonn, Germany

^b also at Kapteyn Institute, University of Groningen, Groningen, The Netherlands

^c School of Physics and Astronomy, University of Leeds, Leeds, United Kingdom

^d Fermi National Accelerator Laboratory, Fermilab, Batavia, IL, USA

^e Pennsylvania State University, University Park, PA, USA

^f Colorado State University, Fort Collins, CO, USA

^g Louisiana State University, Baton Rouge, LA, USA

^h now at Graduate School of Science, Osaka Metropolitan University, Osaka, Japan

ⁱ Institut universitaire de France (IUF), France

^j now at Technische Universität Dortmund and Ruhr-Universität Bochum, Dortmund and Bochum, Germany

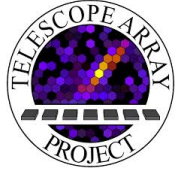
Acknowledgments

The successful installation, commissioning, and operation of the Pierre Auger Observatory would not have been possible without the strong commitment and effort from the technical and administrative staff in Malargüe. We are very grateful to the following agencies and organizations for financial support:

Argentina – Comisión Nacional de Energía Atómica; Agencia Nacional de Promoción Científica y Tecnológica (ANPCyT); Consejo Nacional de Investigaciones Científicas y Técnicas (CONICET); Gobierno de la Provincia de

Mendoza; Municipalidad de Malargüe; NDM Holdings and Valle Las Leñas; in gratitude for their continuing cooperation over land access; Australia – the Australian Research Council; Belgium – Fonds de la Recherche Scientifique (FNRS); Research Foundation Flanders (FWO), Marie Curie Action of the European Union Grant No. 101107047; Brazil – Conselho Nacional de Desenvolvimento Científico e Tecnológico (CNPq); Financiadora de Estudos e Projetos (FINEP); Fundação de Amparo à Pesquisa do Estado de Rio de Janeiro (FAPERJ); São Paulo Research Foundation (FAPESP) Grants No. 2019/10151-2, No. 2010/07359-6 and No. 1999/05404-3; Ministério da Ciência, Tecnologia, Inovações e Comunicações (MCTIC); Czech Republic – GACR 24-13049S, CAS LQ100102401, MEYS LM2023032, CZ.02.1.01/0.0/0.0/16_013/0001402, CZ.02.1.01/0.0/0.0/18_046/0016010 and CZ.02.1.01/0.0/0.0/17_049/0008422 and CZ.02.01.01/00/22_008/0004632; France – Centre de Calcul IN2P3/CNRS; Centre National de la Recherche Scientifique (CNRS); Conseil Régional Ile-de-France; Département Physique Nucléaire et Corpusculaire (PNC-IN2P3/CNRS); Département Sciences de l’Univers (SDU-INSU/CNRS); Institut Lagrange de Paris (ILP) Grant No. LABEX ANR-10-LABX-63 within the Investissements d’Avenir Programme Grant No. ANR-11-IDEX-0004-02; Germany – Bundesministerium für Bildung und Forschung (BMBF); Deutsche Forschungsgemeinschaft (DFG); Finanzministerium Baden-Württemberg; Helmholtz Alliance for Astroparticle Physics (HAP); Helmholtz-Gemeinschaft Deutscher Forschungszentren (HGF); Ministerium für Kultur und Wissenschaft des Landes Nordrhein-Westfalen; Ministerium für Wissenschaft, Forschung und Kunst des Landes Baden-Württemberg; Italy – Istituto Nazionale di Fisica Nucleare (INFN); Istituto Nazionale di Astrofisica (INAF); Ministero dell’Università e della Ricerca (MUR); CETEMPS Center of Excellence; Ministero degli Affari Esteri (MAE), ICSC Centro Nazionale di Ricerca in High Performance Computing, Big Data and Quantum Computing, funded by European Union NextGenerationEU, reference code CN_00000013; México – Consejo Nacional de Ciencia y Tecnología (CONACYT) No. 167733; Universidad Nacional Autónoma de México (UNAM); PAPIIT DGAPA-UNAM; The Netherlands – Ministry of Education, Culture and Science; Netherlands Organisation for Scientific Research (NWO); Dutch national e-infrastructure with the support of SURF Cooperative; Poland – Ministry of Education and Science, grants No. DIR/WK/2018/11 and 2022/WK/12; National Science Centre, grants No. 2016/22/M/ST9/00198, 2016/23/B/ST9/01635, 2020/39/B/ST9/01398, and 2022/45/B/ST9/02163; Portugal – Portuguese national funds and FEDER funds within Programa Operacional Factores de Competitividade through Fundação para a Ciência e a Tecnologia (COMPETE); Romania – Ministry of Research, Innovation and Digitization, CNCS-UEFISCDI, contract no. 30N/2023 under Romanian National Core Program LAPLAS VII, grant no. PN 23 21 01 02 and project number PN-III-P1-1.1-TE-2021-0924/TE57/2022, within PNCDI III; Slovenia – Slovenian Research Agency, grants P1-0031, P1-0385, I0-0033, N1-0111; Spain – Ministerio de Ciencia e Innovación/Agencia Estatal de Investigación (PID2019-105544GB-I00, PID2022-140510NB-I00 and RYC2019-027017-I), Xunta de Galicia (CIGUS Network of Research Centers, Consolidación 2021 GRC GI-2033, ED431C-2021/22 and ED431F-2022/15), Junta de Andalucía (SOMM17/6104/UGR and P18-FR-4314), and the European Union (Marie Skłodowska-Curie 101065027 and ERDF); USA – Department of Energy, Contracts No. DE-AC02-07CH11359, No. DE-FR02-04ER41300, No. DE-FG02-99ER41107 and No. DE-SC0011689; National Science Foundation, Grant No. 0450696, and NSF-2013199; The Grainger Foundation; Marie Curie-IRSES/EPLANET; European Particle Physics Latin American Network; and UNESCO.

The Telescope Array Collaboration



R.U. Abbasi¹, T. Abu-Zayyad^{1,2}, M. Allen², J.W. Belz², D.R. Bergman², F. Bradfield³, I. Buckland², W. Campbell², B.G. Cheon⁴, K. Endo³, A. Fedynitch^{5,6}, T. Fujii^{3,7}, K. Fujisue^{5,6}, K. Fujita⁵, M. Fukushima⁵, G. Furlich², Z. Gerber², N. Globus⁸, T. Hanaoka⁹, W. Hanlon², N. Hayashida¹⁰, H. He^{11*}, K. Hibino¹⁰, R. Higuchi¹¹, D. Ikeda¹⁰, D. Ivanov², S. Jeong¹², C.C.H. Jui², K. Kadota¹³, F. Kakimoto¹⁰, O. Kalashev¹⁴, K. Kasahara¹⁵, Y. Kawachi³, K. Kawata⁵, I. Kharuk¹⁴, E. Kido⁵, H.B. Kim⁴, J.H. Kim², J.H. Kim^{2†}, S.W. Kim^{12‡}, R. Kobo³, I. Komae³, K. Komatsu¹⁶, K. Komori⁹, A. Korochkin¹⁷, C. Koyama⁵, M. Kudenko¹⁴, M. Kuroiwa¹⁶, Y. Kusumori⁹, M. Kuznetsov¹⁴, Y.J. Kwon¹⁸, K.H. Lee⁴, M.J. Lee¹², B. Lubsandorzhiiev¹⁴, J.P. Lundquist^{2,19}, H. Matsushita³, A. Matsuzawa¹⁶, J.A. Matthews², J.N. Matthews², K. Mizuno¹⁶, M. Mori⁹, S. Nagataki¹¹, K. Nakagawa³, M. Nakahara³, H. Nakamura⁹, T. Nakamura²⁰, T. Nakayama¹⁶, Y. Nakayama⁹, K. Nakazawa⁹, T. Nonaka⁵, S. Ogio⁵, H. Ohoka⁵, N. Okazaki⁵, M. Onishi⁵, A. Oshima²¹, H. Oshima⁵, S. Ozawa²², I.H. Park¹², K.Y. Park⁴, M. Potts², M. Przybylak²³, M.S. Pshirkov^{14,24}, J. Remington²⁸, C. Rott², G.I. Rubtsov¹⁴, D. Ryu²⁵, H. Sagawa⁵, N. Sakaki⁵, R. Sakamoto⁹, T. Sako⁵, N. Sakurai⁵, S. Sakurai³, D. Sato¹⁶, K. Sekino⁵, T. Shibata⁵, J. Shikita³, H. Shimodaira⁵, H.S. Shin^{3,7}, K. Shinozaki²⁶, J.D. Smith², P. Sokolsky², B.T. Stokes², T.A. Stroman², H. Tachibana³, K. Takahashi⁵, M. Takeda⁵, R. Takeishi⁵, A. Taketa²⁷, M. Takita⁵, Y. Tameda⁹, K. Tanaka²⁸, M. Tanaka²⁹, M. Teramoto⁹, S.B. Thomas², G.B. Thomson², P. Tinyakov^{14,17}, I. Tkachev¹⁴, T. Tomida¹⁶, S. Troitsky¹⁴, Y. Tsunesada^{3,7}, S. Udo¹⁰, F. Urban³⁰, A.G. Ureña³⁰, M. Vrábel²⁶, D. Warren¹¹, K. Yamazaki²¹, Y. Zhezher^{5,14}, Z. Zundel², and J. Zvirzdin²

¹ Department of Physics, Loyola University-Chicago, Chicago, Illinois 60660, USA

² High Energy Astrophysics Institute and Department of Physics and Astronomy, University of Utah, Salt Lake City, Utah 84112-0830, USA

³ Graduate School of Science, Osaka Metropolitan University, Sugimoto, Sumiyoshi, Osaka 558-8585, Japan

⁴ Department of Physics and The Research Institute of Natural Science, Hanyang University, Seongdong-gu, Seoul 426-791, Korea

⁵ Institute for Cosmic Ray Research, University of Tokyo, Kashiwa, Chiba 277-8582, Japan

⁶ Institute of Physics, Academia Sinica, Taipei City 115201, Taiwan

⁷ Nambu Yoichiro Institute of Theoretical and Experimental Physics, Osaka Metropolitan University, Sugimoto, Sumiyoshi, Osaka 558-8585, Japan

⁸ Institute of Astronomy, National Autonomous University of Mexico Ensenada Campus, Ensenada, BC 22860, Mexico

⁹ Graduate School of Engineering, Osaka Electro-Communication University, Neyagawa-shi, Osaka 572-8530, Japan

¹⁰ Faculty of Engineering, Kanagawa University, Yokohama, Kanagawa 221-8686, Japan

¹¹ Astrophysical Big Bang Laboratory, RIKEN, Wako, Saitama 351-0198, Japan

¹² Department of Physics, Sungkyunkwan University, Jang-an-gu, Suwon 16419, Korea

¹³ Department of Physics, Tokyo City University, Setagaya-ku, Tokyo 158-8557, Japan

¹⁴ Institute for Nuclear Research of the Russian Academy of Sciences, Moscow 117312, Russia

¹⁵ Faculty of Systems Engineering and Science, Shibaura Institute of Technology, Minumaku, Tokyo 337-8570, Japan

¹⁶ Academic Assembly School of Science and Technology Institute of Engineering, Shinshu University, Nagano, Nagano 380-8554, Japan

¹⁷ Service de Physique Théorique, Université Libre de Bruxelles, Brussels 1050, Belgium

¹⁸ Department of Physics, Yonsei University, Seodaemun-gu, Seoul 120-749, Korea

¹⁹ Center for Astrophysics and Cosmology, University of Nova Gorica, Nova Gorica 5297, Slovenia

²⁰ Faculty of Science, Kochi University, Kochi, Kochi 780-8520, Japan

²¹ College of Science and Engineering, Chubu University, Kasugai, Aichi 487-8501, Japan

²² Quantum ICT Advanced Development Center, National Institute for Information and Communications Technology, Koganei, Tokyo 184-8795, Japan

²³ Doctoral School of Exact and Natural Sciences, University of Łódź, Łódź, Łódź 90-237, Poland

²⁴ Sternberg Astronomical Institute, Moscow M.V. Lomonosov State University, Moscow 119991, Russia

²⁵ Department of Physics, School of Natural Sciences, Ulsan National Institute of Science and Technology, UNIST-gil, Ulsan 689-798, Korea

²⁶ Astrophysics Division, National Centre for Nuclear Research, Warsaw 02-093, Poland

²⁷ Earthquake Research Institute, University of Tokyo, Bunkyo-ku, Tokyo 277-8582, Japan

²⁸ Graduate School of Information Sciences, Hiroshima City University, Hiroshima, Hiroshima 731-3194, Japan

²⁹ Institute of Particle and Nuclear Studies, KEK, Tsukuba, Ibaraki 305-0801, Japan

³⁰ *CEICO, Institute of Physics, Czech Academy of Sciences, Prague 182 21, Czech Republic*

Acknowledgments

The Telescope Array experiment is supported by the Japan Society for the Promotion of Science (JSPS) through Grants-in-Aid for Priority Area 431, for International Collaborative Research 24KK0064, for Specially Promoted Research JP21000002, for Scientific Research (S) JP19104006, for Transformative Research Areas (A) JP25H01294, for Specially Promoted Research JP15H05693, for Scientific Research (S) JP19H05607, for Scientific Research (S) JP15H05741, for Science Research (A) JP18H03705, for Young Scientists (A) JPH26707011, and for Fostering Joint International Research (B) JP19KK0074, by the joint research program of the Institute for Cosmic Ray Research (ICRR), The University of Tokyo; by the Pioneering Program of RIKEN for the Evolution of Matter in the Universe (r-EMU); by the U.S. National Science Foundation awards PHY-1806797, PHY-2012934, PHY-2112904, PHY-2209583, PHY-2209584, and PHY-2310163, as well as AGS-1613260, AGS-1844306, and AGS-2112709; by the National Research Foundation of Korea (2017K1A4A3015188, 2020R1A2C1008230, and RS-2025-00556637); by the Ministry of Science and Higher Education of the Russian Federation under the contract 075-15-2024-541, IISN project No. 4.4501.18, by the Belgian Science Policy under IUAP VII/37 (ULB), by National Science Centre in Poland grant 2020/37/B/ST9/01821, by the European Union and Czech Ministry of Education, Youth and Sports through the FORTE project No. CZ.02.01.01/00/22_008/0004632, and by the Simons Foundation (00001470, NG). This work was partially supported by the grants of the joint research program of the Institute for Space-Earth Environmental Research, Nagoya University and Inter-University Research Program of the Institute for Cosmic Ray Research of University of Tokyo. The foundations of Dr. Ezekiel R. and Edna Watis Dumke, Willard L. Eccles, and George S. and Dolores Doré Eccles all helped with generous donations. The State of Utah supported the project through its Economic Development Board, and the University of Utah through the Office of the Vice President for Research. The experimental site became available through the cooperation of the Utah School and Institutional Trust Lands Administration (SITLA), U.S. Bureau of Land Management (BLM), and the U.S. Air Force. We appreciate the assistance of the State of Utah and Fillmore offices of the BLM in crafting the Plan of Development for the site. We thank Patrick A. Shea who assisted the collaboration with much valuable advice and provided support for the collaboration's efforts. The people and the officials of Millard County, Utah have been a source of steadfast and warm support for our work which we greatly appreciate. We are indebted to the Millard County Road Department for their efforts to maintain and clear the roads which get us to our sites. We gratefully acknowledge the contribution from the technical staffs of our home institutions. An allocation of computing resources from the Center for High Performance Computing at the University of Utah as well as the Academia Sinica Grid Computing Center (ASGC) is gratefully acknowledged.

* Presently at: Purple Mountain Observatory, Nanjing 210023, China

† Presently at: Physics Department, Brookhaven National Laboratory, Upton, NY 11973, USA

‡ Presently at: Korea Institute of Geoscience and Mineral Resources, Daejeon, 34132, Korea

§ Presently at: NASA Marshall Space Flight Center, Huntsville, Alabama 35812, USA